

To Boil and Egg: Substrate Binding Affects Critical Stability in Thermal Unfolding of Proteins

By:

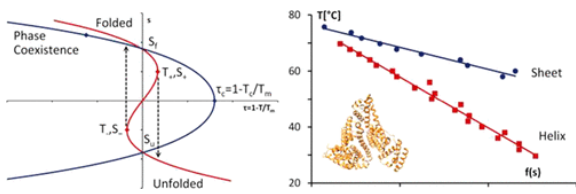
Rohanah Hussain¹, Charlotte S Hughes¹, Tamás Jávorfí¹, Giuliano Siligardi¹, Paul Williams² & Boyan B. Bonev^{2*}

¹ Diamond Light Source Ltd., Harwell Science and Innovation Campus, Chilton, Didcot, Oxfordshire, OX11 0DE, UK;

² School of Life Sciences, University of Nottingham, Queen's Medical Centre, Nottingham NG7 2UH, UK;

Abstract

Thermal unfolding of proteins is used extensively in screening of drug candidates because molecular interactions with ligands and substrates affect strongly protein stability, transition temperature, and cooperativity. We use synchrotron radiation circular dichroism to monitor the thermal evolution of secondary structure in proteins as they approach the melting point and the impact of substrate on their thermal behavior. Using Landau free energy expansion, we quantify transition strength and proximity to a critical point through the relative separation τ_+ between the transition temperature T_m and the spinodal T_+ , obtained from the equation of state. The weakest transition was observed in lysozyme with $\tau_+ = -0.0167$ followed by holo albumin with $\tau_+ = -0.0208$ with the strongest transition in monomeric apo albumin $\tau_+ = -0.0242$. A structural transition at 45 °C in apo albumin leads to a noncooperative melt with $\tau_+ = -0.00532$ and amyloidogenic increase in beta content.



Introduction

Mapping the interactions between proteins and ligands, substrates or other functional partners is of great value to understanding protein function, as well as in development of pharmaceutical compounds. Biochemical and molecular methods based on molecular recognition, such as affinity chromatography and two hybrid tools often involve tagging of proteins and/or partners.¹ NMR methods often require stable isotope incorporation.² Thermal analysis by calorimetry,³ circular dichroism⁴ or other biophysical methods,⁵ widely used in screens of compound libraries, does not involve labelling and relies on the observation that the thermal stability of proteins is usually enhanced in the presence of interaction partners. In such approaches molecular interactions can be observed through changes in the protein unfolding temperatures, which are often altered in the presence of co-factors or other ligands. Molecular interaction screens have been developed and are used widely to pair up proteins with small molecule partners in drug development and many other applications.⁶

Thermal unfolding is the collapse of protein structure through its inability to accommodate thermal fluctuations, which increase in magnitude with temperature and diverge at the transition. The ability of proteins to retain their structure is enhanced by molecular contacts that form during protein-ligand, protein-substrate or protein-protein interactions and confer additional stability to protein structure. We propose that the structure of apo-proteins responds to temperature gradually and unfolds with a weak, less cooperative transition closer to a critical point. (Figure 1 left) Substrate or ligand binding leads to a more stable complex, more resilient to heating, which melts with a stronger and more cooperative transition, away from a critical point. (Figure 1 right)

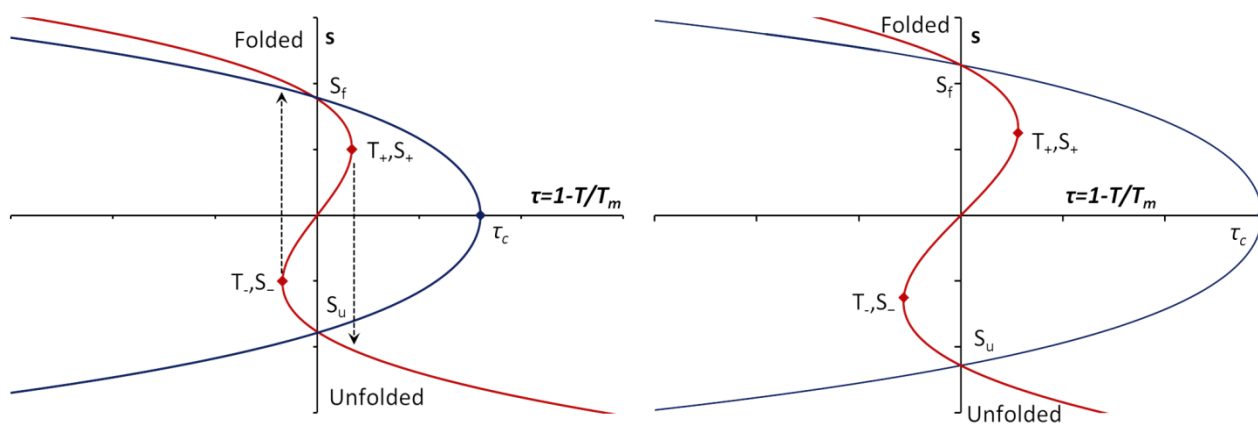


Figure 1: Equation of state (red) showing helical order parameter, s , dependence on reduced temperature $\tau = 1 - T/T_m$. The points (T_+, s_+) are spinodals, which can be reached in thermal evolution of metastable systems before collapse of the fold. In proteins undergoing reversible unfolding the two spinodals give rise to hysteresis by approaching T_+ on heating and T_- on cooling. The coexistence curve (blue) crosses $s = 0$ at the reduced critical temperature $\tau_c = 1 - T_c/T_m$. Order parameters at the transition are s_f and s_u at the folded/unfolded states of the protein, respectively. Apo-proteins (left) unfold with lower τ and ΔG than holo-proteins (right).

Thermal denaturation of proteins is commonly quantified by fitting CD at a single wavelength to the Gibbs-Helmholtz equation:³⁻⁴

$$\Delta G = \Delta H \left(1 - \frac{T}{T_m}\right) - \Delta C_p \left[(T_m - T) + T \ln \left(\frac{T}{T_m}\right) \right] \quad (1)$$

and obtaining T_m as the denaturation temperature at midpoint of change between folded and unfolded state. C_p is the isobaric heat capacity of the system and its change, ΔC_p , and that in enthalpy, ΔH , across the transition are usually reported in calorimetric studies. We introduce a dimensionless reduced temperature $\tau = 1 - \frac{T}{T_m}$ describing the normalised distance from the transition and expression (1) reads:

$$\Delta G = \Delta H(\tau) - \Delta C_p [T_m \tau + T \ln(1 - \tau)] \quad (1')$$

We describe changes in protein structure by introducing a thermodynamic order parameter, which relates to the fractional content of a specific secondary structure component. Such order parameter is related to the molar contribution of hydrogen bonding, g_n , to protein secondary structure:

$$s = \frac{1}{G_0} \sum_1^N g_n \quad (2)$$

The α -helical fraction is roughly monotonic with temperature below the thermal melt temperature and is normalised to the range [1,0] between folded and unfolded states.

We use a simple model, based on a Landau free energy series expansion at T_m in terms of this structural parameter.⁷ Following Morrow and co-workers⁸ and Jahnig⁹ we write the Gibbs free energy as a truncated Landau series expansion in terms of s near the melting temperature T_m :

$$G = G_0 \left[\frac{s^4}{4} + \alpha(T - T_c) \frac{s^2}{2} + \beta(T - T_m)s \right] \quad (3)$$

where $\alpha, \beta < 0$, T_c is the critical temperature and T_m is the transition temperature as described in eq. 1. We have also considered that in our case $s > 0$ in all physical states. The equation of state is obtained by minimising G with respect to s :

$$\frac{\partial G}{\partial s} = s^3 + \alpha(T - T_c)s + \beta(T - T_m) = 0 \quad (4)$$

In first order phase transitions two spinodal points mark the vanishing second derivatives of G and we obtain from the positive spinodal: (Figure 1)

$$\alpha = \frac{3s_+^2}{T_c - T_+} \quad \text{and} \quad \beta = \frac{2s_+^3}{T_+ - T_m} \quad (5)$$

For $T_m < T_c$ the transition is of first order and for $T_m > T_c$ the melt occurs continuously and the transition is of second order. Considering first order transitions, we rewrite the equation of state as:

$$T = T_+ + \frac{T_m - T_+}{2} \left[3 \left(\frac{s - s_+}{s_+} \right)^2 + \left(\frac{s - s_+}{s_+} \right)^3 \right] \quad (6)$$

which describes a linear correlation between the temperature of the system T and a function

$$f(s) = 3 \left(\frac{s - s_+}{s_+} \right)^2 + \left(\frac{s - s_+}{s_+} \right)^3 \quad (7)$$

of the structural parameter s with slope proportional to the distance between the melting point T_m and the spinodal temperature T_+ and intercept equal to the spinodal temperature.^{8a} The relative separation $\tau_+ = 1 - \frac{T_+}{T_m}$ between T_m and the spinodals $T_{s\pm}$ (also related to the critical temperature T_c , at which ΔG vanishes) is a normalised temperature metric, quantifying the strength of the transition and its proximity to a critical point. Such parameter allows comparison of protein unfolding to any other first order transition, such as in lipid membranes,^{8a} liquid-solid, Curie transitions,⁷ etc.

Experimental

Human serum albumin (HSA), essentially globulin free (lipidated) and essentially fatty acid free and globulin free (delipidated), and hens' egg lysozyme were purchased from Sigma-Aldrich. Each protein was dissolved in phosphate buffer 10mM pH 7.5 to a final concentration of 0.5 – 0.6 mg/ml.

Synchrotron radiation circular dichroism:

SRCD far UV experiments were performed using a nitrogen-flushed Module B end-station spectrophotometer at B23 Synchrotron Radiation CD Beamline at the Diamond Light Source ¹⁰ with bandwidth 1.1 nm, integration time of 1 s, 1 nm digital resolution, 39 min/min scan speed with 0.02 cm pathlength Suprasil cell (Hellma Ltd). For thermal stability, spectra were measured every 2° or 5°C over a temperature range between 20°C and 90°C for HSA and Lysozyme. Reversibility was monitored by measuring the spectrum at 20°C after cooling from 90°C with 30 minutes incubation time. The results obtained were processed using CDApps ¹¹ with T_m calculated using Boltzmann equation using OriginPro™. Secondary structure estimation from CD spectra was carried out using CDApps using Continll algorithm ¹².

Linear fitting of secondary structure content and calculations in obtaining the equation of state were carried out in Excel (Microsoft). Molecular structure visualization was done using UCSF Chimera ¹³.

Results and Discussion

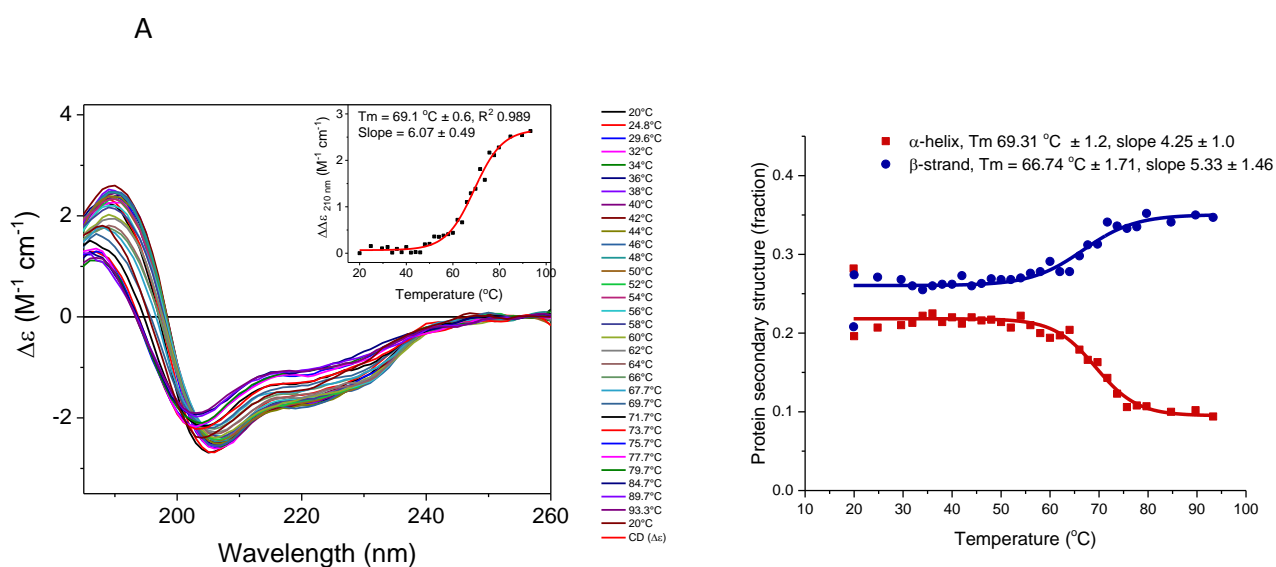
To illustrate our approach we use synchrotron radiation circular dichroism (SRCD) and monitor the effects of thermal fluctuations on the unfolding of a well-characterised soluble protein, hen egg lysozyme. We then apply the analysis to compare the thermal stability of human serum albumin (HSA) in delipidated form and as the fatty acid-stabilised protein.

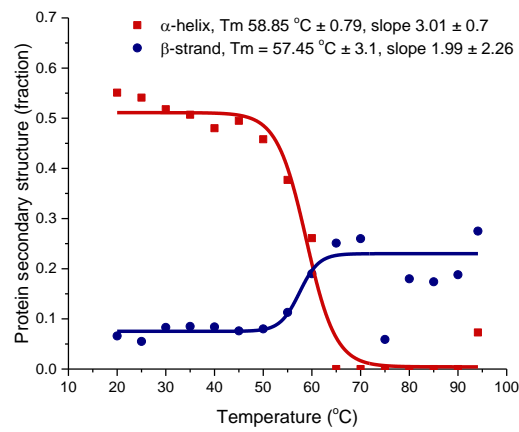
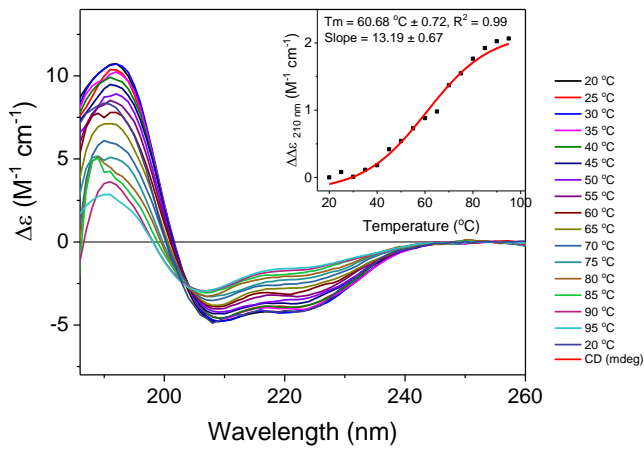
Boltzmann analysis

The study of protein conformational changes by circular dichroism (CD) spectroscopy as a function of heat was conducted by measuring the far-UV CD spectra in the 185-250nm region at various temperatures from 20 to 90°C at 2 or 5°C interval. The far-UV CD spectra permitted protein secondary structure estimation (SSE) in terms of α -helix, β -turn, β -strand and irregular (or unordered) content that can be carried out using several known algorithms such as Continll ¹⁴, Selcon ¹⁵, CDDSTR ¹⁶ and BestSel ¹⁷ to cite the most commonly used. The plot of CD intensity at fixed wavelength versus temperature was used to calculate the melting temperature T_m by fitting the sigmoidal curve with the Boltzmann equation ^{4,18}. Unfolding temperatures T_m obtained from CD intensity at 210 nm were 71.0±1.4°C for holo-HSA, 60.7±0.7°C for apo-HSA and

69.1±0.6°C for lysozyme respectively. Considering this elevation in T_m , fatty acid-saturated holo-HSA appeared more resistant to thermal denaturation than apo-HSA but a direct comparison to lysozyme cannot be made using T_m alone (figures 2A, 2B and 2C). By contrast, the ratio of $\Delta H/\Delta S$ obtained from the slope of the plot in $\Delta\epsilon(210)$ around the transition in holo-HSA, 17.8±1.2, indicates lower cooperativity compared to apo-HSA, 13.2±0.7. Thermal unfolding in lysozyme was even more cooperative than that in either form of HSA with $\Delta\epsilon(210)$ slope around the transition of 6.1±0.5, likely the result of stabilizing role of disulphide bridges.

Similarly, Boltzmann analysis was carried out on the α -helical and β -strand components estimated using Continll for SSE of the thermal denaturation process of the three proteins (holo-HAS, apo-HSA and Lysozyme). The results show that in holo-HSA, the α -helical T_m (68.9±1.2°C) was lower than that of the β -strand components (73.1±1.4°C) (figure. 2A), whereas for apo-HSA, both α -helix and β -strand components showed a similar T_m of 58.9±0.8°C. However, the thermal denaturation profile of the two components in the apo-HSA suggested a more cooperative thermal denaturation process as both slope transitions were small and steep (Fig. 2B). For Lysozyme, on the other hand, a cooperative thermal denaturation process was observed in both α -helix and β -strand components with the β -strand component exhibiting a lower thermal transition temperature than that of the α -helix conformation (Fig. 2C).





C

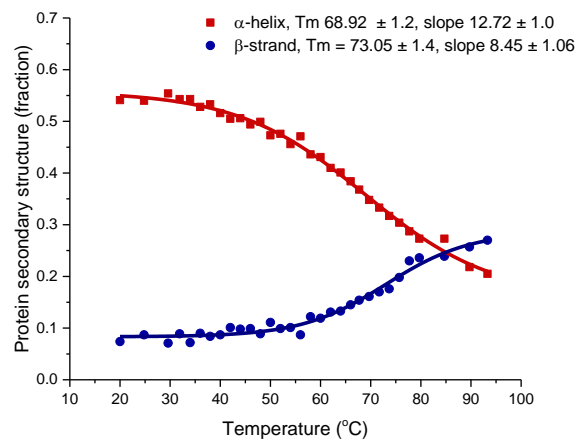
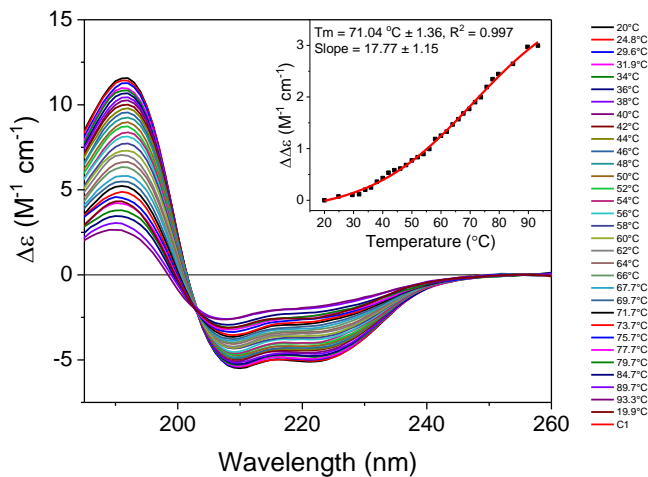


Figure 2: Far UV CD spectra (left); α -helix and β -strand components (right) of (A) Lysozyme, (B) apoHSA and (C) holoHSA as a function of thermal denaturation

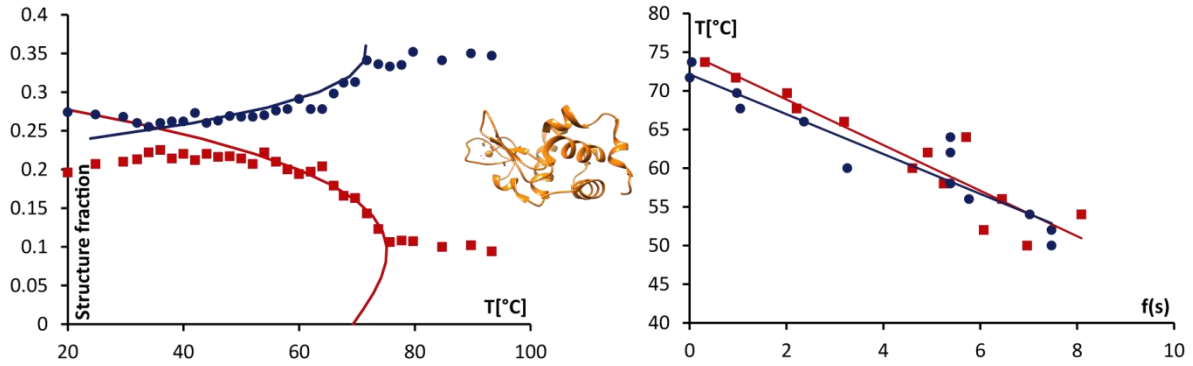
Landau free energy analysis

The interpretation of protein unfolding in terms of thermal fluctuations is illustrated first for lysozyme. (Figure 3C) The protein is stable at temperatures as high as 50°C, above which we observe an accelerated with temperature decline in helical content. The melt, as reported from Boltzmann analysis of helical content occurs at $T_m=69.3\pm 1.2^\circ\text{C}$ and fitting the temperature to $f(s)$ using Equation 6, reveals first order melt with positive spinodal at $T_+=75.0\pm 2.9^\circ\text{C}$, $s_+=0.094$ ($\tau_+=-0.0167\pm 0.00021$). Beta component in lysozyme remains largely independent of temperature up to 50°C, above which it increases gradually alongside the decline in helix and remains invariant above $T_m=66.74\pm 1.7^\circ\text{C}$. Using Equation 6, we obtain the positive

spinodal temperature at $T_{\pm}=71.6\pm 2.0^{\circ}\text{C}$ and $\tau_{\pm}=-0.0143\pm 0.00019$. The similar values of τ_{\pm} in the melting of helix and sheet suggest a common mechanism and the possibility of amyloidogenic conversion of helix to sheet on approach to the melt.

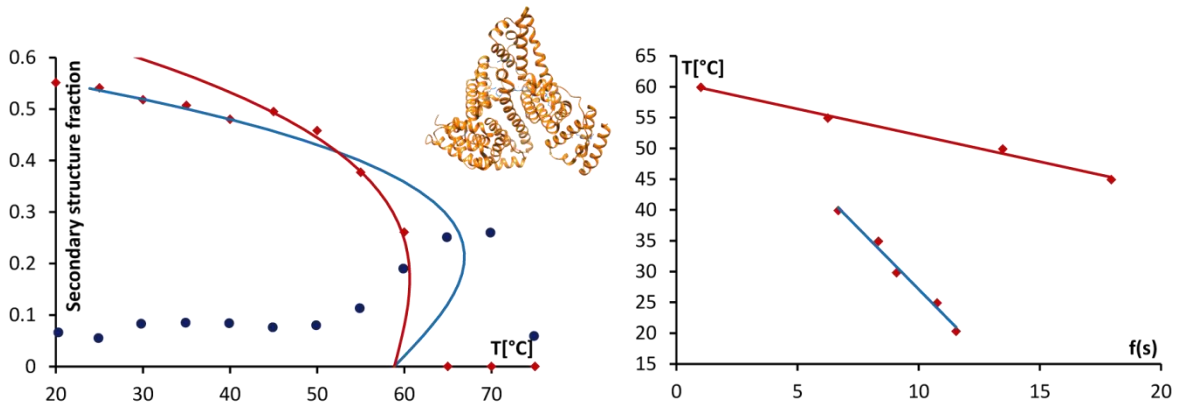
A

Lysozyme



B

apo HSA



C

holo HSA

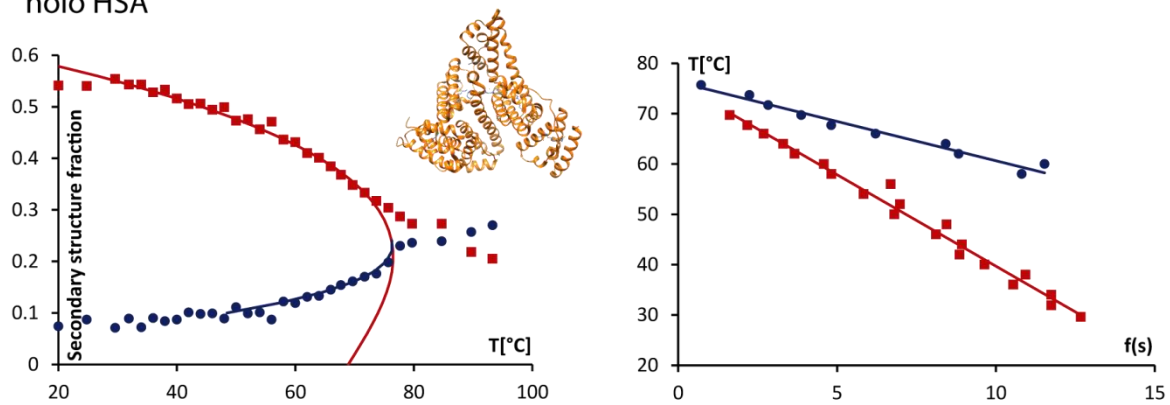


Figure 3: Helical content in A) lysozyme; inset – lysozyme (PDB ID:5K7O)¹⁹; B) apo-HSA, C) holo-HSA as a function of temperature with equations of state (left); insets – HSA (PDB ID:5ID7)²⁰; and, right: linear fits of T vs. $f(s) = 3 \left(\frac{s-s_+}{s_+} \right)^2 + \left(\frac{s-s_+}{s_+} \right)^3$ for each state, used in obtaining the equations of state. Helical content is shown in red squares, while sheet is shown in blue circles with corresponding colours for the equations of state; in B) the low temperature (monomer) equation of state for the helical melt is shown in blue while the high temperature aggregated state is in red. The low fraction and insensitivity of beta component to temperature in the monomeric state and, in part in the aggregated state of apo HSA do not permit reliable fitting of its thermal behaviour.

We investigate the impact of substrate association on thermal stability of HSA in its delipidated apo form and in fatty acid-saturated holo state. SRCD-monitored temperature response of apo-HSA reveals an abrupt shift in trend between 40 and 45°C, (Figure 3, top) which has been reported as onset of aggregation above this temperature.²¹ To quantify this change we analyse the data below 40°C and above 45°C separately as T vs. $f(s)$, according to equation 6 (Figure 3, bottom) and using the value of $T_m=60^\circ\text{C}$ obtained from fitting $\Delta\epsilon(210)$. The two linear fits reveal distinct temperature response below and above 40°C with spinodals for the low temperature state below 40°C at $T_+=67.0\pm 2.7^\circ\text{C}$, $s_+=0.213$ and $\tau_+=-0.0242\pm 0.00032$ and in high temperature, above 45°C, as $T_+=60.7\pm 0.6^\circ\text{C}$, $s_+=0.170$ with $\tau_+=-0.00532\pm 0.00007$. Using these parameters we calculate the equations of state for HSA melting below 40°C and above 45°C and these are plotted alongside the experimental melts in Figure 3B (right) in blue and red, respectively. The decrease in spinodal temperature from 67°C to 61°C, reduction in Δs from 0.213 to 0.170 and 4.6-fold decrease in τ_+ across the aggregation point between 40 and 45°C reveal weakening in the first order character of the transition in the aggregated state. This reveals a switch from tight and cooperative temperature response by the HSA monomer to a less cooperative melt dominated by weakened internal protein cohesion and intermolecular interactions during aggregation. Indeed, small angle neutron scattering measurements have reported an aggregation process in apo-HSA, which takes place at approximately 45°C,²¹ while the Boltzmann analysis of the SRCD thermal melts following $\Delta\epsilon(210)$ shows a single melting transition at 60°C.

In lipidated HSA protein structure is stabilised by multiple contacts with the fatty acids, which elevates the helical T_m to $68.9 \pm 1.2^\circ\text{C}$, determined from the Boltzmann analysis of helical unfolding. Spinodal decomposition analysis reveals the positive spinodal at $T_+ = 76.4 \pm 2.2^\circ\text{C}$, $s_+ = 0.209$ and $\tau_+ = -0.0208 \pm 0.00013$ (Figure 3). Despite elevation in T_m , we observe decrease in both τ_+ and spinodal order Δs_\pm (as well as the corresponding ΔG) in the lipidated form, which reveals a stronger and more cooperative transition in the monomeric low temperature state of apo HSA compared to the lipidated holo HSA. This is the result of disruption of the apo phase by an aggregation process, which leads to a premature structural collapse in the apo form.

One particular observation is that protein denaturation analysis by Boltzmann fitting reports lysozyme unfolding as a stronger, more cooperative transition by comparison to HSA, while Landau free energy expansion analysis ranks the two melts in the opposite order. We interpret this as the result of setting the reference in Boltzmann analysis to a state of the protein with a different fold, while the Landau free energy expansion considers changes in protein structure only within the folded state and with reference to the total energy associated with forming a particular secondary structure type. The former case, therefore, bears the assumption that protein unfolding is only partial and that part of energy remains associated with residual original structure. The free energy expansion model treats the unfolding process as the result of thermal fluctuation that gradually weakens the fold within a complete structural state naïve to the high temperature unfolded conformation and any secondary structure it may contain.

Conclusion

We propose a theoretical framework for the analysis of protein thermal denaturation, monitored by SRCD or other experimental tools capable of following changes in protein structure. In this approach the temperature behaviour of individual secondary structure components is analysed using Landau free energy expansion to obtain spinodal parameters as characteristics of the unfolding transition. This analysis permits quantitative comparison between the unfolding characteristics in proteins with different thermal behaviour, which uses a unified absolute temperature scale referenced to the individual critical point of

each protein. Guided by conventional Boltzmann analysis in obtaining T_m , the method is comparatively insensitive to accurate determination of T_m , as the separation between T_m and T_+ depends only weakly on T_m and is normalised by the absolute value of T_m in the reduced measure τ_+ . Akin to Boltzmann analysis, this approach permits analysis of thermal behaviour of individual structural elements, such as helices and sheet.

The method is also sensitive to changes in protein structure and interactions within the folded state and it's application is demonstrated on well-characterised proteins lysozyme and HSA. Thermal unfolding of lysozyme is of first order, closer to critical point and less cooperative than unfolding of monomeric apo or holo HSA with $\tau_+ = -0.0167$, $\tau_+ = -0.0242$ and $\tau_+ = -0.0208$, respectively. Curiously, holo HSA unfolds closer to a critical point than monomeric apo HSA, despite its higher T_m . Our approach reveals a structural transition in apo HSA, associated with aggregation and amyloidogenic increase in sheet, which interrupts the normal thermal evolution of apo HSA and leads to a non-cooperative melt at lower temperature and 4.6-fold lower $\tau_+ = -0.00532$ (Table 1). The method is robust and sensitive to complex thermal behaviour that is further affected by intermolecular interactions during substrate or ligand binding and is developed as an assay for observing protein interactions at the molecular level, including molecular interactions in membranes.

	Lysozyme	apo-HSA aggregating	apo-HSA monomeric	holo-HSA
T_m [°C]	69.3±1.2	58.9±0.8		68.9±1.2
T_+ [°C]	75.0±2.9	60.7±0.6	67.0±2.7	76.0±0.8
τ_+	-0.0167±0.00021	-0.00532±0.00007	-0.0242±0.00032	-0.0208±0.00013
s_+	0.094±0.001	0.170±0.001	0.213±0.001	0.209±0.001

Table 1: Reduced spinodal temperature $\tau_+ = 1 - \frac{T_+}{T_m}$ and order s_+ ; apo-protein (blue) and holo-protein (orange) pairs. Uncertainties in T_m were obtained from Boltzmann analysis, in T_+ from linear regression analysis and in τ from the cumulative relative errors in T_m and T_+ .

Acknowledgements

The work was funded by the Medical Research Council grant MR/N010477/1 to PW&BB and the Biotechnology and Biological Sciences Research Council, UK grant BB/N010426/1 to BB. We like to thank Diamond Light Source for access to B23 beamline (SM15146, SM13634, SM12545, SM12923) and Lab 22.

References

1. Kambe, T.; Correia, B. E.; Niphakis, M. J.; Cravatt, B. F., Mapping the Protein Interaction Landscape for Fully Functionalized Small-Molecule Probes in Human Cells. *J. Am. Chem. Soc.* **2014**, *136* (30), 10777-10782.
2. Rajesh, S.; Overduin, M.; Bonev, B. B., NMR of Membrane Proteins: Beyond Crystals. *Adv. Exp. Med. & Biol.* **2016**, *922*, 29-42.
3. Brandts, J. F.; Lin, L. N., Study of strong to ultratight protein interactions using differential scanning calorimetry. *Biochemistry* **1990**, *29* (29), 6927-6940.
4. Greenfield, N. J., Using circular dichroism collected as a function of temperature to determine the thermodynamics of protein unfolding and binding interactions. *Nat. Prot.* **2006**, *1* (6), 2527-2535.
5. Niesen, F. H.; Berglund, H.; Vedadi, M., The use of differential scanning fluorimetry to detect ligand interactions that promote protein stability. *Nat. Prot.* **2007**, *2* (9), 2212-2221.
6. Huber, K. V. M.; Olek, K. M.; Muller, A. C.; Tan, C. S. H.; Bennett, K. L.; Colinge, J.; Superti-Furga, G., Proteome-wide drug and metabolite interaction mapping by thermal-stability profiling. *Nat. Meth.* **2015**, *12* (11), 1055-1057.
7. Landau, L., The theory of phase transitions. *Nature* **1936**, *138*, 840-841.
8. (a) Bonev, B. B.; Morrow, M. R., Effect of pressure on the dimyristoylphosphatidylcholine bilayer main transition. *Phys. Rev. E* **1997**, *55* (5), 5825-5833; (b) Morrow, M. R.; Whitehead, J. P., A phenomenological model for lipid-protein bilayer with critical mixing. *Biochim. Biophys. Acta* **1988**, *941* (2), 271-277.
9. Jahnig, F., Critical effects from lipid-protein interaction in membranes. 1. Theoretical description. *Biophys. J.* **1981**, *36* (2), 329-345.
10. (a) Javorfi, T.; Hussain, R.; Myatt, D.; Siligardi, G., Measuring circular dichroism in a capillary cell using the b23 synchrotron radiation CD beamline at diamond light source. *Chirality* **2010**, *22 Suppl 1*, E149-53; (b) Hussain, R.; Javorfi, T.; Siligardi, G., Circular dichroism beamline B23 at the Diamond Light Source. *J Synchrotron Radiat* **2012**, *19* (Pt 1), 132-5.
11. Hussain, R.; Benning, K.; Javorfi, T.; Longo, E.; Rudd, T. R.; Pulford, B.; Siligardi, G., CDApps: integrated software for experimental planning and data processing at beamline B23, Diamond Light Source. *J. Synchr. Radiation* **2015**, *22* (2), 465-468.
12. Sreerama, N.; Woody, R. W., On the analysis of membrane protein circular dichroism spectra. *Protein Sci.* **2004**, *13* (1), 100-12.
13. Pettersen, E. F.; Goddard, T. D.; Huang, C. C.; Couch, G. S.; Greenblatt, D. M.; Meng, E. C.; Ferrin, T. E., UCSF Chimera--a visualization system for exploratory research and analysis. *J Comput. Chem.* **2004**, *25* (13), 1605-12.
14. Provencher, S. W.; Glockner, J., Estimation of globular protein secondary structure from circular dichroism. *Biochemistry* **1981**, *20* (1), 33-37.
15. Sreerama, N.; Woody, R. W., Estimation of protein secondary structure from circular dichroism spectra: Comparison of CONTIN, SELCON, and CDSSTR methods with an expanded reference set. *Analytical Biochemistry* **2000**, *287* (2), 252-260.
16. Vanstokkum, I. H. M.; Spoelder, H. J. W.; Bloemendal, M.; Vangrondelle, R.; Groen, F. C. A., Estimation of protein secondary structure and error analysis from circular dichroism spectra. *Anal. Biochem.* **1990**, *191* (1), 110-118.
17. Micsonai, A.; Wien, F.; Kernya, L.; Lee, Y. H.; Goto, Y.; Refregiers, M.; Kardos, J., Accurate secondary structure prediction and fold recognition for circular dichroism spectroscopy. *Proc. Natl. Acad. Sci. U.S.A.* **2015**, *112* (24), E3095-E3103.
18. Singleton, D. G.; Hussain, R.; Siligardi, G.; Kumar, P.; Hrdlicka, P. J.; Berova, N.; Stulz, E., Increased duplex stabilization in porphyrin-LNA zipper arrays with structure dependent exciton coupling. *Org. & Biomol. Chem.* **2016**, *14* (1), 149-157.
19. de la Cruz, M. J.; Hattne, J.; Shi, D.; Seidler, P.; Rodriguez, J.; Reyes, F. E.; Sawaya, M. R.; Cascio, D.; Weiss, S. C.; Kim, S. K.; Hinck, C. S.; Hinck, A. P.; Calero, G.; Eisenberg, D.; Gonen, T., Atomic-resolution structures from fragmented protein crystals with the cryoEM method MicroED. *Nat. Meth.* **2017**, *14* (4), 399-402.
20. Sekula, B.; Ciesielska, A.; Rytczak, P.; Koziółkiewicz, M.; Bujacz, A., Structural evidence of the species-dependent albumin binding of the modified cyclic phosphatidic acid with cytotoxic properties. *Biosci. Rep.* **2016**, *36* (3).

21. Heller, W. T., Comparison of the Thermal Denaturing of Human Serum Albumin in the Presence of Guanidine Hydrochloride and 1-Butyl-3-methylimidazolium Ionic Liquids. *J. Phys. Chem. B* **2013**, *117* (8), 2378-2383.